Acta Neuropathol (2015) 129:279–295
DOI 10.1007/s00401-014-1372-1

ORIGINAL PAPER

Perivascular microglia promote blood vessel disintegration in the ischemic penumbra

Valérie Jolivel · Frank Bicker · Fabien Binamé · Robert Ploen · Stefanie Keller · René Gollan · Betty Jurek · Jérôme Birkenstock · Laura Poisa-Beiro · Julia Bruttger · Verena Opitz · Serge C. Thal · Ari Waisman · Tobias Bäuerle · Michael K. Schäfer · Frauke Zipp · Mirko H. H. Schmidt

Received: 2 June 2014 / Revised: 1 December 2014 / Accepted: 1 December 2014 / Published online: 13 December 2014

Abstract The contribution of microglia to ischemic cortical stroke is of particular therapeutic interest because of the impact on the survival of brain tissue in the ischemic penumbra, a region that is potentially salvable upon a brain infarct. Whether or not tissue in the penumbra survives critically depends on blood flow and vessel perfusion. To study the role of microglia in cortical stroke and blood vessel stability, CX3CR1$^{+/GFP}$ mice were subjected to transient middle cerebral artery occlusion and then microglia were investigated using time-lapse two-photon microscopy in vivo. Soon after reperfusion, microglia became activated in the stroke penumbra and started to expand cellular protrusions towards adjacent blood vessels. All microglia in the penumbra were found associated with blood vessels within 24 h post reperfusion and partially fully engulfed them. In the same time frame blood vessels became permissive for blood serum components. Migration assays in vitro showed that blood serum proteins leaking into the tissue provided molecular cues leading to the recruitment of microglia to blood vessels and to their activation. Subsequently, these perivascular microglia started to eat up endothelial cells by phagocytosis, which caused an activation of the local endothelium and contributed to the disintegration of blood vessels with an eventual break down of the blood brain barrier. Loss-of-microglia-function studies using CX3CR1$^{GFP/GFP}$ mice displayed a decrease in stroke size and a reduction in the extravasation of contrast agent into the brain penumbra as measured by MRI. Potentially, medication directed at inhibiting microglia activation within the first day after stroke could stabilize blood vessels in the penumbra, increase blood flow, and serve as a valuable treatment for patients suffering from ischemic stroke.

V. Jolivel and F. Bicker contributed equally as first but M. K. Schäfer, F. Zipp and M. H. H. Schmidt contributed equally as last authors.

Electronic supplementary material The online version of this article (doi:10.1007/s00401-014-1372-1) contains supplementary material, which is available to authorized users.

V. Jolivel · R. Ploen · R. Gollan · B. Jurek · J. Birkenstock · L. Poisa-Beiro · F. Zipp
Department of Neurology, Focus Program Translational Neuroscience (FTN), Rhine Main Neuroscience Network (rmn2), Johannes Gutenberg University, University Medical Center, Mainz, Germany

F. Bicker · S. Keller · V. Opitz · M. H. H. Schmidt (✉)
Molecular Signal Transduction Laboratories, Institute for Microscopic Anatomy and Neurobiology, Focus Program Translational Neuroscience (FTN), Rhine Main Neuroscience Network (rmn2), Johannes Gutenberg University, University Medical Center, Langenbeckstr. 1, 55131 Mainz, Germany
e-mail: mirko.schmidt@unimedizin-mainz.de

F. Binamé
Molecular Cell Biology, Department of Biology, Johannes Gutenberg University, Mainz, Germany

J. Bruttger · A. Waisman
Institute for Molecular Medicine, Focus Program Translational Neuroscience (FTN), Rhine Main Neuroscience Network (rmn2), Johannes Gutenberg University, University Medical Center, Mainz, Germany

S. C. Thal · M. K. Schäfer
Department of Anesthesiology, Focus Program Translational Neuroscience (FTN), Rhine Main Neuroscience Network (rmn2), Johannes Gutenberg University, University Medical Center, Mainz, Germany

T. Bäuerle
Institute of Radiology, University Medical Center, Erlangen, Germany

Keywords Blood-brain barrier · Endothelial cell · Ischemic stroke · Microglia · Middle cerebral artery occlusion

Introduction

Ischemic stroke ranks among the most common causes of mortality and adult disability in industrialized countries [38]. Astrup et al. [5] observed in 1977 that the reduction of cerebral blood flow to under a critical limit created dysfunctional regions in the brain, as the occlusion of a cerebral artery causes the abrupt deprivation of oxygen and nutrients leading to impaired ionic balance, neuronal depolarization, and massive cell death [1, 27, 43]. The region in which blood flow drops to below 20 % of preocclusion values is designated as the core of the lesion. Basic tissue metabolism cannot be maintained and cell loss is fast and irreversible [21]. In the surrounding penumbra, blood flow ranges between 25 and 50 % of preocclusion values [17, 20]. The damaged tissue there remains in a critical state for hours and days, during which a further reduction of blood flow leads to cell death but an increase to functional recovery and repair [39]. Consequently, an evolvement of tissue damage in the ischemic penumbra is observed, which can be separated in three phases. First, the acute phase, which takes place in the first minutes upon stroke and is characterized by massive cell loss in the core region. Subsequently, the subacute phase lasts for about 6–24 h and is characterized by an expansion of tissue damage from the core into the surrounding healthy tissue of the penumbra. Finally, the delayed injury phase, which lasts for days to weeks and is characterized by secondary phenomena, such as vasogenic edema and inflammation [21]. The temporal and spatial progression of ischemic cell damage and its dependence on blood flow suggest that modulators of blood vessel integrity affect the magnitude of damaged tissue and the speed at which damage occurs.

Key elements in stroke are brain resident mononuclear phagocytes termed microglia, which are part of the innate immune system and are considered as orchestrators of the inflammatory response in the CNS [61]. Under physiological conditions these cells exhibit a small cell body bearing thin and ramified processes that are continuously palpating the brain parenchyma [9, 51]. Upon ischemic stroke microglia become activated and adopt a de-ramified morphology with retracted processes and enlarged cell bodies. Several studies have demonstrated the involvement of microglia in brain ischemia [22, 23] but their contribution to the progression of stroke remains under debate. The transplantation of microglia into a lesioned area reduced the infarct volume and improved functional recovery [28, 29]; however, less invasive loss-of-microglia-function studies such as the genetic knock-out of CX3CR1 led to a reduction of the infarct volume by 56 % [12].

Putatively, the analysis of different microglia subpopulations and a diverging impact on the breakdown of the blood–brain barrier (BBB) [67] cause these antagonistic observations, and in order to explore the mechanism, dynamics, and the orchestration of microglia-dependent events in ischemic stroke, we performed kinetic investigations and intravital two-photon laser-scanning microscopy of CX3CR1$^{+/GFP}$ mice subjected to reversible middle cerebral artery occlusion (MCAO). In a time frame corresponding to the subacute to early delayed phase of stroke, we observed the engulfment of blood vessels by microglia in the penumbra, which culminated in the phagocytic degradation of blood vessels and the active breakdown of the BBB leading to the conclusion that microglia actively participate in the transfer of stroke-induced injury in healthy neighboring tissue by the disassembly of blood vessels and the resulting decrease in blood flow in the ischemic penumbra.

Materials and methods

Middle cerebral artery occlusion (MCAO)

MCAO was performed by application of the intraluminal suture technique using C57BL/6J or B6.129P-CX3CR1^{tm1Litt}/J mice (The Jackson Laboratory, Bar Harbor, ME, USA), referred to in the text as CX3CR1$^{+/GFP}$ (heterozygous, no phenotype) or CX3CR1$^{GFP/GFP}$ (homozygous, CX3CR1 knock-out) mice, respectively. Previously, C57BL/6J and heterozygous animals have been shown to exhibit similar infarct sizes [13]. Briefly, after a midline incision at the neck, a filament with a silicon-coated tip (Doccol, Sharon, MA, USA) was advanced from the external carotid artery into the lumen of the internal carotid artery until it blocked the origin of the left middle cerebral artery. MCAO was verified by a drop in laser Doppler flow (Perimed, Järfälla, Sweden) of at least 80 % of the baseline. Sham animals were obtained by inserting the filament into the internal carotid artery without insertion into the middle cerebral artery. The filament was removed 1 h after MCAO in order to allow reperfusion. Animal procedures were performed under the supervision of authorized investigators in accordance with the European Union normative for care and use of experimental animals. Mice were anesthetized by isoflurane (AbbVie, Ludwigshafen, Germany) applied in oxygen (3 l/min) and received a subcutaneous injection of Rimadyl (Pfizer, Berlin, Germany) as an analgesic. Body temperature was maintained at 37.5 ± 0.5 °C by a homeothermic blanket. Finally, animals were placed for 2 h in a recovery chamber maintained at 33 °C after subcutaneous

administration of 500 µL of 0.9 % saline. Only animals that exhibited a score ≥1 in neurological evaluations [36] were used for experimental analyses.

Intravital microscopy

Mice were anesthetized with 1.5 % isoflurane (AbbVie) applied in oxygen/nitrous oxide (2:1, 3 l/min) using a face mask and then tracheotomized and continuously respirated with a Harvard Apparatus advanced safety respirator (Hugo Sachs, March-Hugstetten, Germany). The cerebral cortex was exposed by careful removal of the skull bone of the left hemisphere. The brain was superfused with isotonic Ringer solution that was continuously exchanged by a peristaltic pump. An agarose patch (0.5 % in 0.9 % NaCl solution) was installed on the exposed brain surface to reduce heartbeat and breathing artifacts. The depth of anesthesia was controlled by continuous CO_2 measurements of exhaled gas and recorded with a CI-240 Microcapnograph (Columbus Instruments, Columbus, OH, USA). Prior to preparation the vasculature was stained by intravenous injection of rhodamine–dextran 1.5 h before imaging (Sigma, Hamburg, Germany). Experiments were performed using a specialized two-photon laser-scanning microscope (TriMscope; LaVision BioTec, Bielefeld, Germany) equipped with a Ti:Sa laser (MaiTai, SpectraPhysics, Darmstadt, Germany) set at 850 nm and a synchronously pumped optical parametric oscillator (APE, Berlin, Germany) set at 1,100 nm for simultaneous imaging of two colors. XYZ stacks were typically collected within a scan field of 300 × 300 µm at 512 × 512 pixel resolution and a *z*-plane distance of 2 µm at a frequency of 400 or 800 Hz. The penumbra region in two-photon imaging studies was defined by preliminary MCAO studies (ligation time 1 h, $n = 16$). One day after reperfusion mice were killed and the location and size of the infarct analyzed by cresyl violet staining. MCAO yielded reproducible results and allowed prediction of the localization of core and penumbra of stroke. Further, mice were scored for motor deficits and only animals that exhibited a score ≥1 in neurological evaluations [36] were used for two-photon imaging.

Immunofluorescence

Mice were anesthetized with ketamine (Ratiopharm, Ulm, Germany) plus xylazine (Bayer Vital, Leverkusen, Germany) and were killed by transcardial perfusion with 4 % paraformaldehyde (PFA) at 1, 3, 6, 12, 24, and 72 h post reperfusion. These mice received an intravenous injection of 100 µl of 20 mg/ml Evans blue (Sigma) 30 min before the perfusion. Brains were removed, successively transferred into 15 and 30 % sucrose solution, frozen in cooled isopentane (Applichem, Gatersleben, Germany), and subsequently cryosectioned. Brain sections (20 µm) were incubated overnight with rabbit anti-caveolin-1 (1:250, clone D46G3, Cell Signaling Technology, Cambridge, UK), rat anti-CD31 (clone MEC 13.3, 1:150, BD Biosciences, San Jose, CA, USA), rat anti-CD31/PECAM1 (1:100, Dianova, Hamburg, Germany), rabbit anti-CD68 (1:200, AbD Serotec, Oxford, UK), mouse anti-claudin-5 (1:200, Invitrogen, Carlsbad, CA, USA), rabbit anti-Glut1 (1:100, Merck Millipore, Darmstadt, Germany), goat anti-EGFL7 (1:100, Santa Cruz, La Jolla, CA, USA), rabbit anti-Iba-1 (1:1,000, Wako Chemicals, Richmond, VA, USA), rat anti-ICAM-1 (1:100, clone YN1/1.7.4, BioLegend, San Diego, CA, USA), mouse anti-MAP2 (1:750, Sigma), rat anti-neutrophil (imp-R14, 1:250, Abcam, Cambridge, UK), mouse anti-NF160 (1:300, Sigma), mouse anti-NG2 (1:500, Merck Millipore), rabbit anti-PDGF-B (kindly provided by Carl-Henrik Heldin, LICR, Uppsala University, Sweden), goat anti-podocalyxin (1:200, R&D Systems, Minneapolis, MN, USA), mouse anti-SMA (1:200, Sigma), rabbit anti-VEGF (1:100, Abcam), or rabbit anti-vWF (1:1,000, Dako, Hamburg, Germany) primary antibodies followed by incubation with Alexa Fluor 488-conjugated goat anti-rabbit, Alexa Fluor 568-conjugated goat anti-mouse, anti-rabbit or anti-rat, Alexa Fluor 647-conjugated goat anti-rabbit (Invitrogen), or Alexa 594-conjugated donkey anti-goat (Jackson, Baltimore, PA, USA) secondary antibodies at a dilution of 1:1,000. Cell nuclei were counterstained with 0.5 µg/ml DAPI (Sigma) for 5 min at RT. Images were captured using an SPE confocal microscope (Leica, Mannheim, Germany). 3D reconstruction and analysis were performed using Imaris 8 (Bitplane, Zurich, Switzerland) or ImageJ software v1.41 (National Institute of Health, Bethesda, MD, USA).

In order to analyze BBB breakdown and blood leakage, murine IgG in the brain parenchyma was measured in the cortical stroke region. Deeply anesthetized mice were perfused with 4 % PFA and brain sections prepared on a vibratome (Thermo). Slides were incubated overnight with Alexa Fluor 488-conjugated goat anti-mouse antibody (1:250; Invitrogen) to stain for murine IgG. The next day neurons were identified by rabbit anti-NeuN (1:500; Abcam) as a primary and Alexa Fluor 568-conjugated goat anti-rabbit as a secondary antibody (1:1,000, Invitrogen). Slides were mounted in Immu-Mount (Thermo) and images obtained by an inverted TCS-5 confocal laser-scanning microscope (Leica).

The association of microglia with blood vessels was quantified in fluorescence microscopy images using the Leica Microscope Imaging Software by counting and comparing cells associated and not associated with blood vessels. In order to measure endocytosis of blood vessel components by microglia, immunohistochemical colocalization of the blood vessel marker CD31 and the microglia marker

Iba-1 was quantified using the Imaris 8 software (Bitplane). Thresholds were chosen according to signal intensities and analyzed data represent the percentage of the signal that colocalized above the threshold for each time point.

Magnetic resonance imaging (MRI)

CX3CR1$^{GFP/GFP}$ and wild-type mice underwent MCAO and were killed 6 or 24 h post reperfusion by transcardial perfusion with 4 % PFA solution. The MR contrast agent Gadovist (Bayer) was injected by intravenous injection at 0.2 mmol/kg in all animals, 15 min before being killed. Brains were removed, post-fixed in 4 % PFA and, for MR examinations, processed in 4 % agarose to prevent movement within the scanner. The samples were placed in a mouse whole body coil (Bruker, Ettlingen, Germany) of a dedicated small animal ultra-high-field MR scanner (ClinScan 7 Tesla). Imaging sequences and parameters were chosen as follows: T1-weighted imaging (slices 12, TR 500 ms, TE 9 ms, averages 2, voxel size 0.073 × 0.073 × 0.7 mm^3, acquisition time 5:38 min), diffusion-weighted imaging (DWI, slices 7, TR 8,000 ms, TE 60 ms, averages 1, voxel size 0.234 × 0.234 × 1.0 mm^3, acquisition time 16:16 min) and T2*-weighted imaging (slices 14, TR 983 ms, TE 4 ms, averages 2, voxel size 0.156 × 0.156 × 0.5 mm^3, acquisition time 6:17 min). The volumes (mm^3) of diffusion restriction after MCAO (infarcted areas are displayed as hypointense on maps of the apparent diffusion coefficient, ADC), of local bleeding (displayed as hypointense on maps of T2*-weighted imaging), or the breakdown of the BBB (displayed as hyperintense on T1-weighted imaging) were determined using the Osirix software (Osirix-Foundation, open-source).

Gene expression

BV2 cells [19] were cultured under standard conditions (5 % CO_2 and 95 % humidity) in Dulbecco's modified Eagle's medium (DMEM, Gibco, Karlsruhe, Germany) supplemented with 10 % fetal calf serum and 1 % penicillin/streptomycin. Cells were serum deprived 1 day prior to the experiment and the next day trypsinized, plated on poly-L-lysine (Sigma)-coated dishes, and treated for 6 h with 0.1 or 0.5 % albumin (Sigma), 0.01 or 0.5 % fibrinogen (Merck Millipore), or 5 % fetal calf serum (Sigma). Total RNA was isolated using the RNeasy Mini Kit (Qiagen, Hilden, Germany) and DNAse I treatment (Roche, Mannheim, Germany) performed to avoid contaminations with genomic DNA. The quality of total RNA preparation was confirmed using a Nanodrop 2000c spectrophotometer (Thermo) and cDNA obtained using the Superscript III first strand synthesis system together with random hexamer primers (Invitrogen) according to the manufacturer's guidelines. Primers for quantitative reverse transcriptase polymerase chain reactions (qRT-PCRs) were designed using the Beacon Designer 8 software (Premier Biosoft, Palo Alto, CA, USA) and were subsequently tested for efficiency and specificity. qRT-PCR was performed using the iQ SYBR Green supermix and the iCycler iQ5 device (both BioRad, Hercules, CA, USA). Glyceraldehyde 3-phosphate dehydrogenase (GAPDH) and elongation factor 1 alpha (EF-1 alpha) were used as a housekeeping genes and relative changes in gene expression were determined using the ΔΔCt method [37].

qRT-PCR analyses of matrix metalloprotease 9 (MMP-9) were performed in duplicate using the primers AAGTCTCAGAAGGTGGAT and AATAGGCTTTGTCTTGGTA yielding an amplicon size of 106 bp, a SYBR Green PCR kit (BioRad), and a Lightcycler 480 PCR system (Roche). Absolute copy numbers of MMP-9 were normalized to peptidylprolyl isomerase A (PPIA) as a housekeeping gene. Statistical analyses were performed as described below.

Trans-well migration assays in vitro

Migration of BV2 cells was measured using modified Boyden chambers (8 µm pore size, BD Biosciences) coated with poly-L-lysine. Then 1.5 × 10^5 cells were seeded in 200 µl medium in the upper chamber, while the bottom well contained 600 µl of medium supplemented with albumin (0.1 and 0.5 %), fibrinogen (0.01 and 0.5 %), or fetal calf serum (5 %). Migration was carried out for 6 h and cells were fixed with 4 % PFA. Cells that had migrated to the lower side of the filter were stained with Hoechst 33258 (Sigma) and counted upon image acquisition with an inverted microscope (Leica).

Flow cytometry analyses (FACS)

Mice were deeply anesthetized and perfused with PBS 1 day post reperfusion. Subsequent to the removal of the cerebellum, each brain was separated into an ipsilateral and a contralateral hemisphere. Tissue was dissociated using the "neuronal tissue dissociation kit (P)" (Miltenyi Biotec, Bergisch Gladbach, Germany) according to the manufacturer's instructions. Cells were enriched by a Percoll (Sigma) gradient and prepared for FACS using anti-CD11b-Pe-Cy7 (eBioscience, San Diego, CA, USA), anti-CD45.2-PE (eBioscience), anti-CD68-FITC (Acris Antibodies, San Diego, CA, USA), or anti-CD86 V450 (BD Biosciences) antibodies. Measurements were performed using a FACSCanto II (BD Biosciences) device and data was analyzed using FlowJo v9.6.2 software (Tree Star, Ashland, OR, USA). CD45.2 intermediate and CD11b high cells were considered as microglia.

Statistical analysis

Data were analyzed using Prism5 software (Graphpad, San Diego, CA, USA). Data are presented as mean ± SEM of at least three independent experiments. Statistical analysis of the data was conducted using a non-parametric test (Mann–Whitney or Kruskal–Wallis tests) followed by a Dunn's multiple comparison test. Alternatively, data are presented as mean ± SD and were compared between experimental groups with Wilcoxon Mann–Whitney rank sum tests with *p* values adjusted for each parameter for multiple comparisons by Bonferroni adjustment. Statistical analysis was performed with the Sigma Plot 11 statistical software package (Systat Software Inc., San Jose, CA, USA).

Results

Microglia associate with blood vessels after MCAO

BBB disruption and microglial activation are prominent pathological features of stroke; however, little attention has been paid to the dynamics and kinetics of microglial activation and the implications for blood vessels. In order to address this issue, we applied a mouse model in which the knock-in of GFP into the CX3CR1 gene labels microglia and peripheral macrophages under heterozygous conditions ($CX3CR1^{+/GFP}$) and which serves as a microglia-loss-of-function model under homozygous conditions ($CX3CR1^{GFP/GFP}$). $CX3CR1^{+/GFP}$ mice were subjected to transient MCAO with an occlusion time of 1 h, which was determined as a sufficient time frame to induce cortical damage (Fig. 1a). GFP expression was restricted to Iba-1-positive microglia (Fig. 1b–d). Imaging studies were performed at a tissue depth of 80 µm or deeper as measured from the tissue surface to reduce imaging artifacts due to the opening of the skull. Brain sections of MCAO-treated mice revealed that the core of the stroke was devoid of microglia and neurons (Fig. 1e), but in the ischemic penumbra, a close association of microglia (Iba-1), blood vessels (CD31), and neurons (MAP2) was observed (Fig. 1f–h). In a time course analysis taken 1–72 h post reperfusion, microglia adjacent to CD31-positive blood vessels displayed hypertrophic characteristics, an elongated shape, and thicker and retracted processes after 1 h (Fig. 1i). The number of cells that displayed an elongated morphology and enlarged cell bodies steadily increased over time (3 h) and microglia began to align with blood vessels in the ischemic hemisphere (Fig. 1j). At 6 h post reperfusion, the ongoing association of microglia with blood vessels in the penumbra resulted in an uneven distribution of microglia in the perilesional tissue (Fig. 1k). After 12 h, perivascular microglia exhibited the characteristic morphology of activated cells and displayed enlarged cell bodies with shortened thick processes that were in direct contact with blood vessels (Fig. 1l). At 24 h post reperfusion an increased number of microglia displayed spherical cell bodies (Fig. 1m). After 72 h a decreased number of blood vessels was observed (Fig. 1n). Quantification of the amount of blood vessel-associated microglia over time displayed a steady increase in perivascular microglia reaching a 2.5-fold increase 24 h and a 3.1-fold increase 72 h post reperfusion as compared to sham-operated mice (Fig. 1o). Costaining of microglia (Iba-1) and smooth muscle cells (SMA; Suppl. Fig. 1a–d) or pericytes (NG2; Suppl. Fig. 1e–h) in the ischemic penumbra 24 h post reperfusion showed that perivascular microglia did not stain positive for either of the latter markers.

Microglia form perivascular clusters upon MCAO

In order to study the dynamics of microglia association with blood vessels upon MCAO, intravital two-photon microscopy was performed in anesthetized $CX3CR1^{+/GFP}$ mice using a cranial window drilled into the skull to analyze the cerebral cortex. At 24 h after reperfusion, evenly distributed, highly ramified microglia were observed in control mice (Fig. 2a). In contrast, microglia in the penumbra of MCAO-treated animals displayed enlarged cell bodies and formed perivascular clusters (Fig. 2b). Time-lapse recordings taken 24 h after reperfusion illustrated "resting microglia", which scanned the brain parenchyma with thin and long processes in control animals (Fig. 2c) but identified activated microglia with enlarged cell bodies and shorter processes in the penumbra (Fig. 2d). As a matter of fact, neighboring groups of microglia protruded their processes towards rhodamine–dextran-labeled blood vessels (Fig. 2e). Individual microglia fully enwrapped small blood vessels as displayed in a 3D reconstruction of a perivascular microglia cell in the penumbra (Fig. 2f).

Blood-derived proteins activate microglia

The engulfment of blood vessels in the ischemic penumbra by microglia raised the question of what are the molecular mechanisms that lead to the recruitment and activation of the local microglia pool. Serum albumin and fibrinogen have been described as proteins leaking into the parenchyma upon BBB breakdown [2, 70]; therefore, we analyzed whether or not these proteins attract microglia upon MCAO. The administration of albumin and fibrinogen to microglial BV2 cells in trans-well migration assays in vitro increased cell migration in a dose-dependent manner (Fig. 3a). Further, albumin and fibrinogen caused an activation of BV2 microglia cells as determined by the upregulation of inflammatory proteins such as the cytokines IL-1β,

IL-6, IL-10, TNF-α, the chemokines MIP-1α and MCP-1, and the chemokine receptor CX3CR1 (Fig. 3b–h). In order to verify the activation of microglia in vivo, CD45.2-intermediate and CD11b-high microglia were isolated from wild-type, sham- or MCAO-treated animals 24 h after surgery and analyzed by FACS. Interestingly, the populations of cells positive for the phagocytosis marker CD68 (16.5-fold) or the co-stimulatory molecule CD86 (55-fold) were elevated in microglia from the ipsilateral hemisphere as compared to those from the contralateral site or control (Fig. 3i, j). Data suggest extravasating serum proteins such as albumin and fibrinogen contribute to the recruitment and activation of microglia subsequent to MCAO.

Phagocytosis of blood vessels by perivascular microglia

The above findings raised the questions of the functional relevance of the association of microglia with blood vessels. Therefore, brain sections of the contralateral (Fig. 4a) or ipsilateral hemisphere of MCAO-treated animals (Fig. 4b) were stained for Iba-1 (microglia) and CD31 (blood vessels). Subsequently, immunostaining and microscopical analysis were performed and orthogonal optical sections were three-dimensionally reconstructed. Perivascular microglia were barely seen in the control situation (Fig. 4a′) but most microglia were found to be associated with blood vessels in the ipsilateral hemisphere upon MCAO (Fig. 4b′). Importantly, the association of microglia with blood vessels was not restricted to individual cells but was observed for almost all microglia. Furthermore, the micromorphology of microglia was different comparing cells derived from the contralateral (Fig. 4c) and the ipsilateral hemisphere (Fig. 4d). In the latter, individual perivascular microglia displayed intracellular vesicles containing CD31-positive particles, suggesting a partial or full uptake of blood vessel-derived endothelial cells (EC). A time course analysis revealed a steady increase in CD31-positive intracellular vesicles in perivascular microglia (Fig. 4e–g). Quantification yielded a massive increase in internalization 24 h (70-fold) and 72 h (115-fold) post reperfusion as compared to sham-operated mice (Fig. 4h). Immunohistochemical staining of the phagocytosis marker CD68 verified that intracellular vesicles were phagosomes (Fig. 4i). To verify that intracellular particles carried EC material, we additionally applied the brain vasculature-specific EC markers Glut-1 (Suppl. Fig. 2a–c), caveolin-1 (Suppl. Fig. 2d–f), claudin-5 (Suppl. Fig. 2g–i), and podocalyxin (Suppl. Fig. 2j–l), which colocalized specifically with CD31 in brain vessels. Indeed, intracellular vesicles in microglia (Iba-1) also stained positive for all four endothelial markers, verifying that blood vessel components were internalized by microglia (Suppl. Fig. 3a–l). Further, no colocalization between perivascular microglia and smooth muscle cells (Suppl. Fig. 1a–d) or pericytes was observed (Suppl. Fig. 1e–h), showing that not these cells but ECs were internalized. Whether microglia phagocytized EC or dying neurons was analyzed by staining for Iba-1 and a combination of the neuronal marker MAP2 plus the neurofilament marker NF160 that marks neuronal processes and filaments. However, no perivascular microglia phagocytizing neuronal debris could be observed (Suppl. Fig. 1i–l), indicating that indeed EC components were taken up by perivascular microglia in the ischemic penumbra.

Perivascular microglia-mediated blood vessel disintegration was followed in real time and in vivo by intravital two-photon microscopy of heterozygous CX3CR1$^{+/GFP}$ mice. At 4 h post reperfusion, we detected the activation of microglia with extensions of individual cells converging towards adjacent blood vessels in the cerebral tissue (Suppl. Movie 1). Long-term measurements starting 4 h post reperfusion and running for approximately 4.5 h revealed the localized and simultaneous recruitment of microglia to blood vessels as soon as 8 h post reperfusion in the ischemic penumbra (Suppl. Movie 2). This involved movements of microglia processes as well as cell bodies (Suppl. Movies 3, 4). At 24 h post reperfusion perivascular microglia started to phagocytize rhodamine–dextran-positive blood vessel components (Suppl. Movie 5), which eventually led to the disintegration of individual tubes (Suppl. Movie 6). Data suggest an MCAO-induced association of microglia with blood vessels, which led to a partial or full phagocytosis of neighboring blood vessel ECs.

Perivascular microglia contribute to the breakdown of the BBB

The findings above raised the question of whether the phagocytosis of EC components affects the respective blood vessels. Under physiological conditions, ECs of healthy vessels are found in a resting mode referred to as phalanx cells. Upon an insult that disrupts the integrity of the EC layer, phalanx cells become activated and may form tip and stalk cells, which display a high degree of plasticity and allow the damaged blood vessel to repair itself through a process termed angiogenesis. Once the damage is fixed, ECs re-enter a quiescent mode [7]. A novel marker expressed in activated ECs is the protein epidermal growth factor-like protein 7 (EGFL7) [49, 60], which we employed here as a marker for the activated endothelium [50] as an alternative to the vascular endothelial growth factor (VEGF). Immunohistochemical staining of brain slices for EGFL7 and the EC activation marker VEGF 24 h post reperfusion showed that both proteins colocalized in brain ECs in the ischemic penumbra (Suppl. Fig. 4a–c). Upregulation of further activation markers such as the platelet-derived growth factor-B (PDGF-B), the von Willebrand

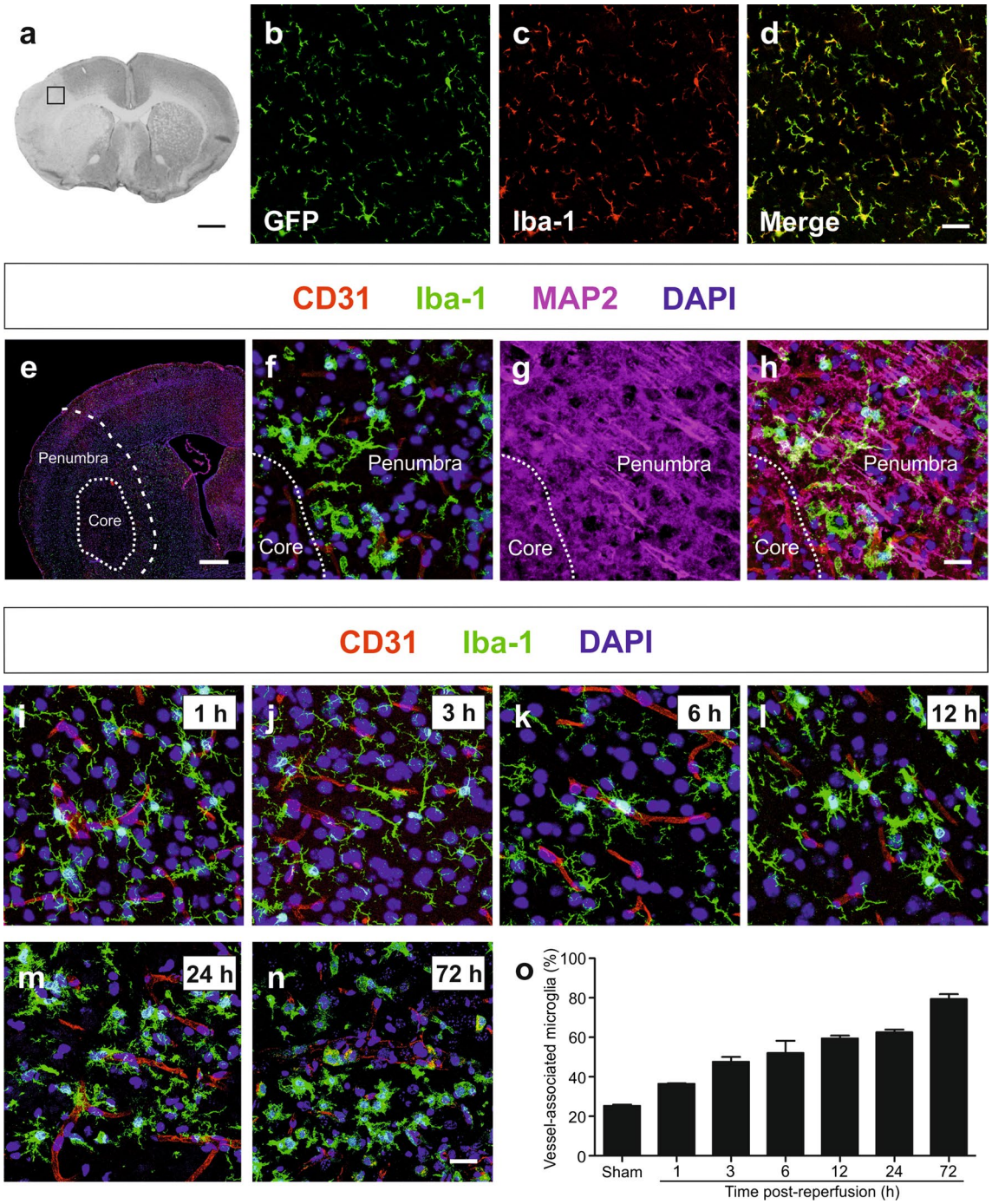

Fig. 1 Microglia associate with the vasculature upon MCAO. **a** Cresyl violet stained murine brain sections 24 h after MCAO. *Box* indicates the region analyzed in subsequent sections. *Bar* represents 1 mm. **b–d** Brain sections derived from CX3CR1-GFP mice were immunostained for Iba-1 to verify co-labeling of microglia by both markers. *Bar* represents 20 µm. **e–h** Murine brain sections 24 h after MCAO. Infarct area including core and penumbra are labeled with *dotted lines*. Iba-1-positive microglia (**e**, **f**, and **h**) as well as MAP2-positive neurons (**g**, **h**) are present in the penumbra but not in the core of the infarct area. *Scale bar* represents 500 µm (**e**) and 10 µm (**h**). **i–n** Brain sections derived from wild-type mice subsequent to transient MCAO at various time points after reperfusion. Microglia cells were identified by Iba-1 and blood vessels by anti-CD31 immunostaining, cell nuclei were counterstained by DAPI. *Bar* represents 25 µm. **o** Quantification of blood vessel-associated and non-associated microglia revealed a steady increase in the amount of perivascular microglia over time post reperfusion ($n \geq 3$)

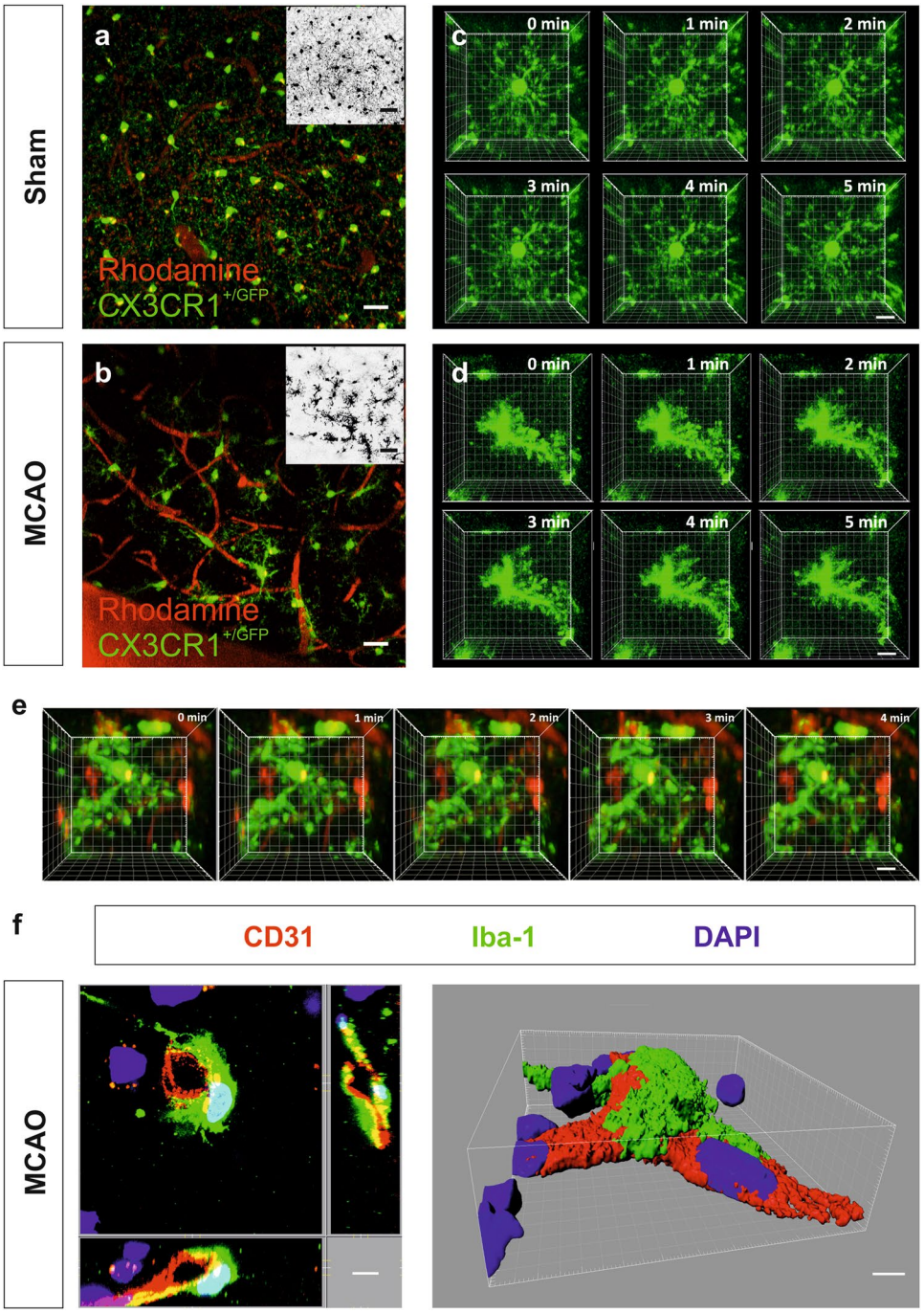

Fig. 2 Microglia form perivascular clusters and engulf blood vessels upon stroke. **a** Two-photon images of the cerebral cortex of CX3CR1$^{+/GFP}$ control (sham operated) or **b** MCAO animals in vivo 24 h post reperfusion. Blood vessels were visualized by perfusion with rhodamine–dextran. *Insets* represent *gray scale* pictures of the same figures to illustrate microglia morphology ($n \geq 10$). *Bar* represents 20 µm and 5 µm (*inset*). **c** Time-lapse recordings identified resting microglia actively palpating the tissue in control animals, while **d** MCAO led to an activation of microglia as displayed by a migratory phenotype and **e** an active association of microglia with rhodamine–dextran-positive blood vessel ($n \geq 10$). *Bars* represent 5 µm. **f** Microglia enwrapped blood vessel in the penumbra 24 h post MCAO as determined by double-immunostaining of Iba-1 (microglia) and CD31 (ECs) followed by orthogonal optical sectioning and a 3D reconstruction. *Bars* represent 5 µm

factor (vWF), or the intercellular adhesion molecule-1 (ICAM-1) [24, 64, 68] verified that indeed ECs of brain vessels in the ischemic penumbra were activated 24 h post MCAO (Suppl. Fig. 4d–l). Brain slides taken from control animals (Fig. 5a–d) or MCAO-treated animals (Fig. 5e–h) were immunohistochemically triple-stained for claudin-5 (blood vessels; Fig. 5a, e), EGFL7 (activated blood vessels; Fig. 5b, f), and Iba-1 (microglia; Fig. 5c, g). Data revealed that perivascular microglia upregulated EGFL7 in adjacent blood vessels 24 h post MCAO (Fig. 5h′). This indicates that ECs in these blood vessels were activated, which is indicative of disintegration of the BBB [69].

In order to determine whether or not perivascular microglia induced a breakdown of the BBB, various hallmarks of this event were analyzed. At 24 and 72 h post reperfusion the expression of MMP-9, a protein described to be involved in stroke BBB turnover [4, 11], increased threefold in the penumbra upon MCAO as compared to sham-treated animals (Fig. 6a). In parallel, staining for extravasated IgG in the cerebral cortex of animals upon MCAO

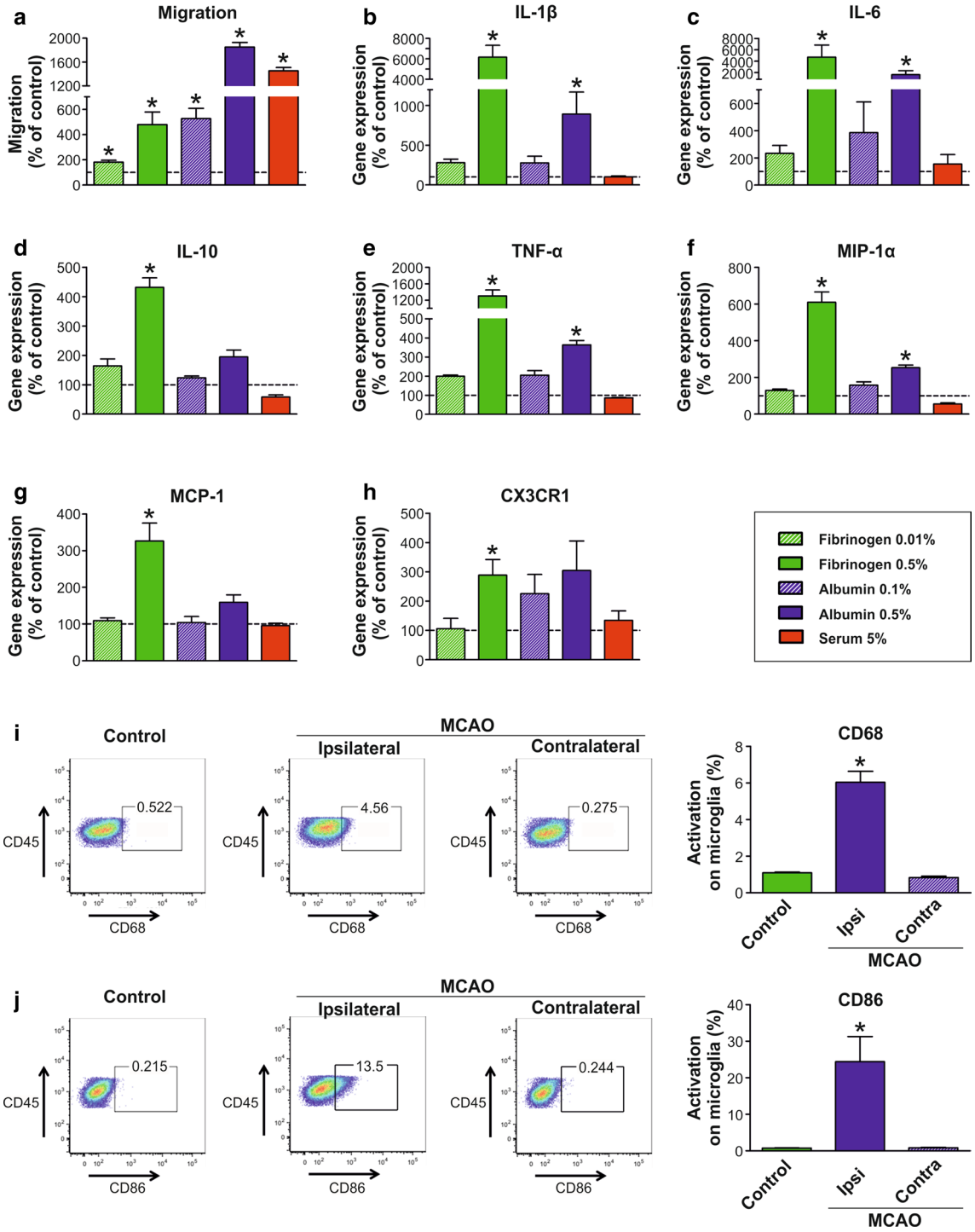

Fig. 3 Extravasating blood serum proteins activate microglia. **a** Trans-well migration assays of microglia cells revealed a dose-dependent stimulation of microglia migration by blood serum albumin, fibrinogen, or fetal calf serum, which served as a positive control. Results are plotted as compared to the migration of unstimulated microglia (mean ± SEM, $n = 4$, $^*p < 0.05$). **b**–**f** Likewise, albumin and fibrinogen caused an activation of microglia cells as determined by qRT-PCR of inflammatory proteins such as **b** IL-1β, **c** IL-6, **d** IL-10, and **e** TNF-α, the chemokines **f** MIP-1α and **g** MCP-1, or **h** the chemokine receptor CX3CR1 (mean ± SEM, $n = 5$, $^*p < 0.05$). **i**, **j** CD45.2-intermediate and CD11b-high microglia were isolated from the brain of control (sham-operated) mice or the contra- as well as the ipsilateral hemisphere of MCAO-treated animals 24 h after surgery. FACS analyses revealed that the phagocytosis marker **i** CD68 and **j** the co-stimulatory molecule CD86 were upregulated 16.5-fold or 55-fold, respectively

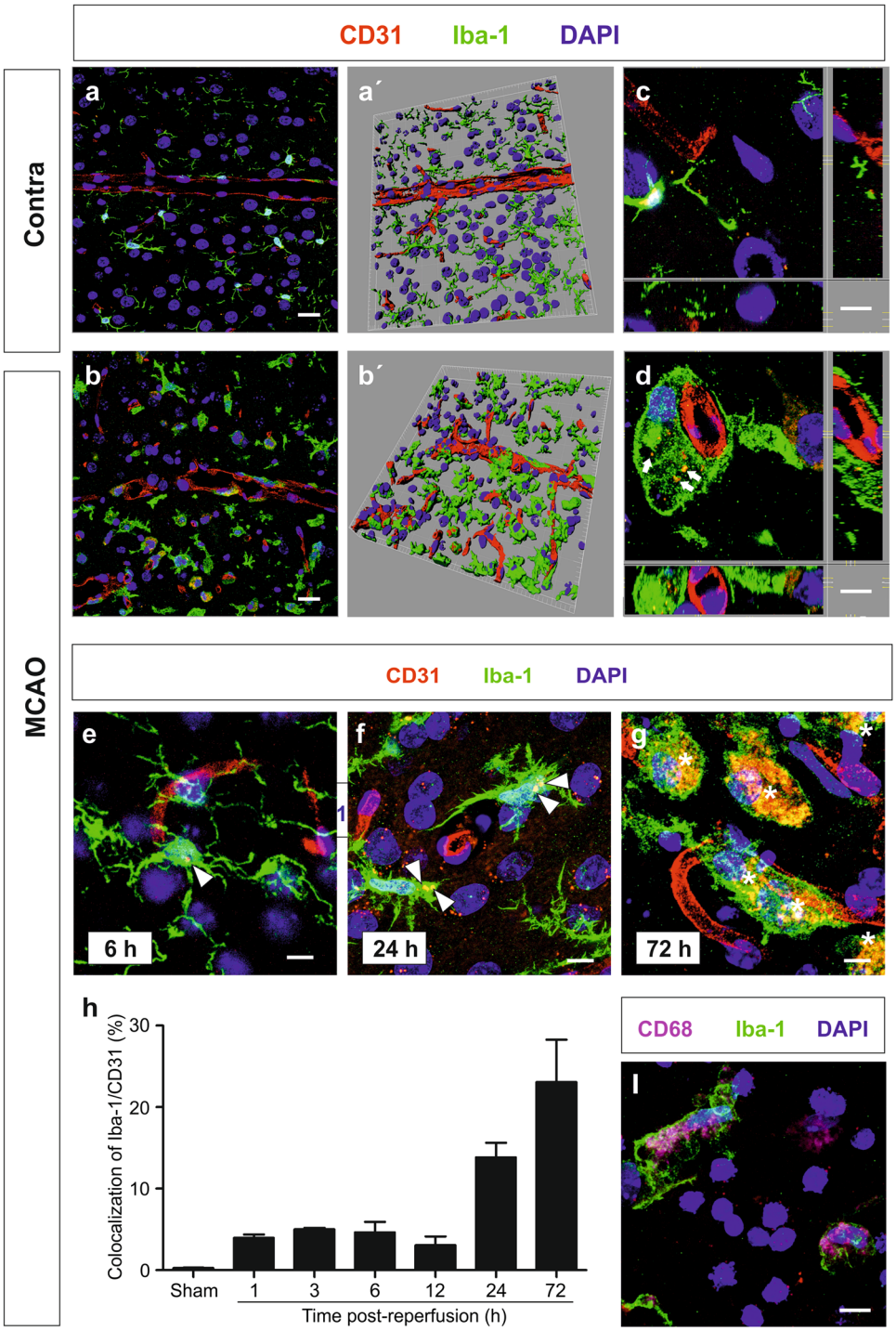

Fig. 4 Perivascular microglia phagocytize blood vessels upon MCAO. **a** Brain slices of the contralateral or **b** ipsilateral hemisphere of MCAO-treated animals were stained for Iba-1 (microglia) and CD31 (ECs). Orthogonal optical sections revealed individual microglia enwrapping and partially digesting blood vessels after stroke. **a′**, **b′** 3D reconstructions indicate an intimate spatial relationship of microglia and blood vessels upon MCAO in the penumbra. *Bars* represent 20 µm. **c**, **d** Higher magnifications of **a** and **b** with **d** displaying CD31-positive vesicles in perivascular microglia suggesting phagocytosis of EC components as indicated by *arrows*. *Bars* represent 10 µm. **e**–**g** Double-staining of microglia for Iba-1 and CD31 (ECs) revealed a steady increase in the amount of CD31-positive intracellular vesicles over time post reperfusion (*arrowheads* and *asterisks*). *Bars* represent 10 µm. **h** Quantification of colocalization (*yellow*, intracellular particles) yielded a 70-fold increase after 24 h and a 115-fold increase 72 h post reperfusion as compared to sham-operated mice. **i** Staining of microglia (Iba-1) for the phagocytosis marker CD68 showed that perivascular microglia were phagocytically active 24 h post reperfusion. *Bars* represent 10 µm

revealed that blood vessels in the ipsilateral hemisphere of the treated animals became much more permissive for blood components such as IgG 24 h after reperfusion as compared to the contralateral hemisphere (Fig. 6b, c). Leakage of IgG occurred in the core and the penumbra as indicated by the diminished immunoreactivity for the neuronal marker NeuN (Fig. 6d). Immunohistochemical analysis and 3D reconstruction revealed that the association of microglia with blood vessels contributed to their disintegration and BBB breakdown as shown by the extravasation of Evans blue in vessels that were still perfused (Fig. 6e, e′). Further, qRT-PCR analysis revealed a threefold increase in the amount of CD11b-positive immune cells in the ipsilateral hemisphere as compared to the contralateral site (Fig. 6f). This is indicative of the activation of the local microglia pool [35] as well as an increased extravasation

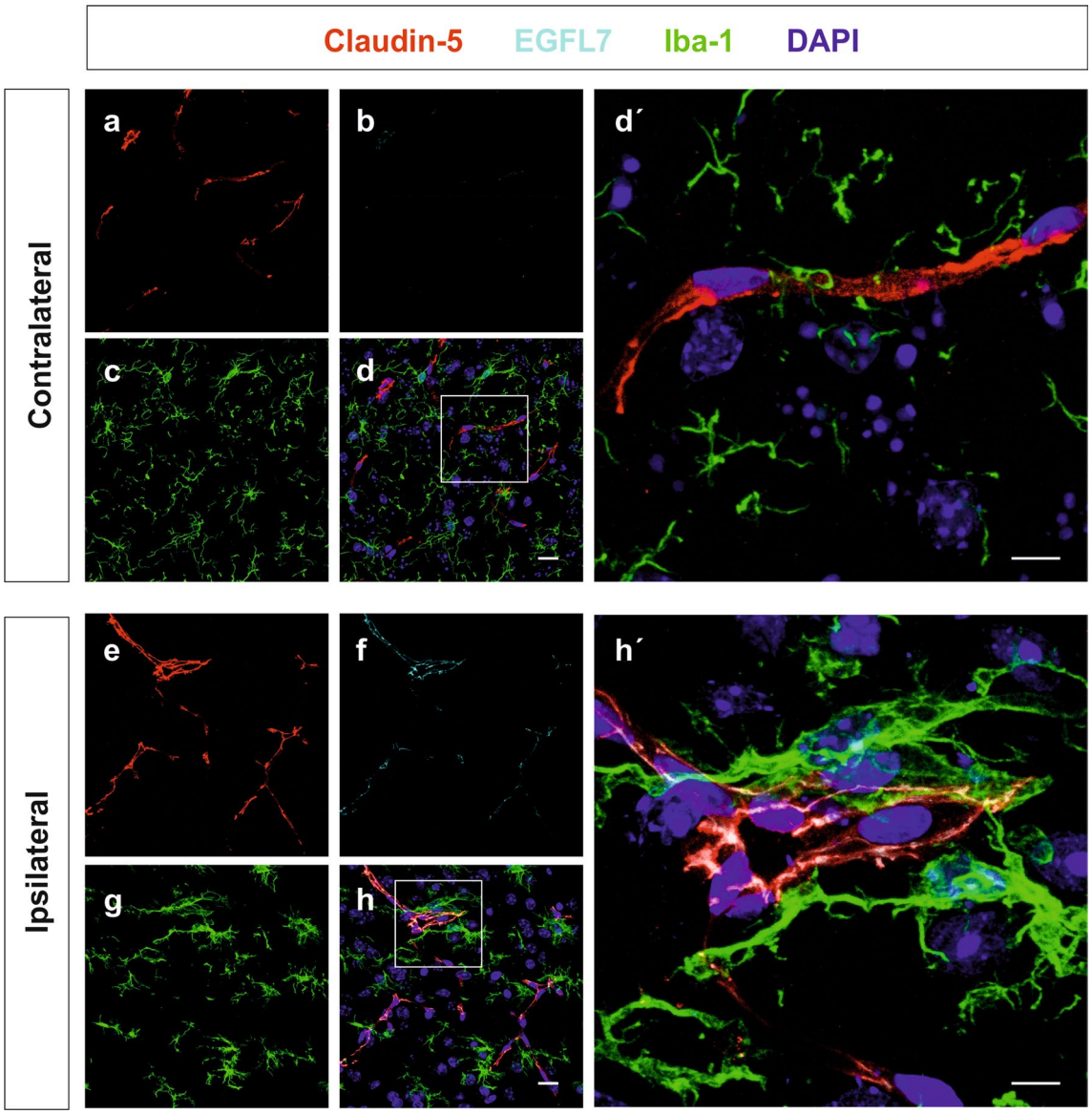

Fig. 5 Perivascular microglia stimulate blood vessel plasticity upon MCAO. Brain slices of MCAO-treated animals were immunohistochemically stained for claudin-5 (ECs), EGFL7 (EC plasticity), and Iba-1 (microglia) on the contralateral (**a**–**d**) and ipsilateral (**e**–**h**) hemisphere 24 h post insult. Cell nuclei were counterstained with DAPI. **d**, **h** Perivascular microglia induced an EC-specific upregulation of the blood vessel plasticity marker EGFL7, indicative of EC activation and BBB breakdown in the penumbra. *Bars* represent 25 µm. **d′**, **h′** Display higher magnifications of the *boxed* regions in the corresponding figures. *Bars* represent 10 µm

of immune cells into the penumbra. In order to validate the latter, we immunohistochemically stained for neutrophils, microglia, and blood vessels in the penumbra of MCAO-treated animals at various times post reperfusion (Fig. 6g–i). Activated perivascular microglia and extravasating neutrophils were observed in the ipsilateral hemisphere in the penumbra 24 h post reperfusion (Fig. 6h). At 72 h post reperfusion, activated microglia and neutrophils were still observed in the penumbra but no tubular structures and only fragments of blood vessels could be detected (Fig. 6i). Data indicate that the blood vessels in the ischemic penumbra disintegrated and were subsequently degraded. The physiological relevance of the above findings was analyzed using CX3CR1$^{GFP/GFP}$ mice harboring microglia that are functionally impaired and therefore suited to perform loss-of-microglia-function studies [12]. MCAO was performed for 1 h and animals were killed 6 and 24 h post reperfusion by transcardial perfusion. At 15 min before being killed mice received an injection of 0.2 mmol/kg Gadovist as a contrast agent in order to quantify leakage of blood vessels in the stroke region. Stroke size and extravasation of contrast agent in the brain penumbra were

measured by ultra-high-field MRI (Fig. 7a). At 24 h post reperfusion loss of microglia function led to a significant ($p < 0.05$) reduction in stroke size of 46.8 % (Fig. 7b) as determined on apparent diffusion coefficient (ADC) maps. Furthermore, extravasation of the contrast agent Gadovist (T1-weighted imaging), representing a breakdown of the BBB, was reduced by 50.4 % (Fig. 7c) in CX3CR1$^{GFP/GFP}$ mice as compared to wild-type animals. At 6 h post reperfusion results showed comparable trends but did not reach significance. Data demonstrate that reduced microglia activity correlates with a decrease in stroke size as well as increased blood vessel integrity.

Discussion

Intravital two-photon microscopy of CX3CR1$^{+/GFP}$ mice in vivo revealed that microglia and peripheral macrophages associated with blood vessels in the ischemic penumbra upon transient MCAO. Microglia exhibited an altered morphology as compared to control cells with larger cell bodies and extensions that were both shorter and thicker [26]. The somata of perivascular microglia were found to fully engulf individual blood vessels in the perilesional tissue within a time frame of 24 h after the ischemic insult. In a related study, microglia were instantly activated in response to an acute microdisruption of the BBB induced by a laser [51]. Resting microglia of control animals repetitively palpated their environment in the cerebral parenchyma with cellular protrusions but microglia adjacent to the lesion switched from an undirected to a directed movement of their cellular extensions towards the damaged area. This culminated in a shielding of blood vessels by microglial processes. However, this study did not elaborate on the subsequent role of microglia in blood vessel disintegration and the implications of this pathological process for the evolvement of tissue damage into the ischemic penumbra.

The clearance of damaged cerebral tissue by microglia has been shown to be essential for neuroregeneration [48] and neuroplasticity [41]. In the current study, we present evidence that perivascular microglia engulf blood vessels and actively perform phagocytosis of EC or subcellular EC-derived particles, as perivascular microglia displayed CD68- and CD31-positive intracellular vesicles upon MCAO. Engulfed blood vessels were still perfused as indicated by erythrocytes within the vascular tube (Fig. 6e), suggesting that ECs were alive and the phagocytized CD31-positive material was not derived from dead cells. Additionally, perivascular microglia exhibited spherical extensions and cups at the extremity of the cellular processes, which have been implicated in the clearance of cellular material by microglia [63, 65]. The disposal of newborn neurons [62], living neural precursor [8], and complete glioma cells [31] by microglia was previously observed upon engulfment, indicating that perivascular microglia are capable of internalizing and degrading EC.

This raises the question of the contribution of the microglia population to phagocytosis in general as microglia are not the only phagocytic cell type detected upon cerebral ischemia in the brain. As a matter of fact, an influx of circulating monocytes and macrophages has been reported to occur 24 h after the insult and may persist for up to 1 week [18]. Schilling et al. analyzed mice harboring genetically GFP-labeled blood leukocytes for parenchymal leukocyte invasion into the brain in response to stroke at various time points. The study demonstrated that microglia predominantly exerted a phagocytic activity against neuronal cell debris in the penumbra 24 h after transient MCAO, which matches the time frame in which most of our analyses were performed [59]. Nevertheless, Schilling et al. did not emphasize the role of perivascular microglia in the phagocytosis of EC and the physiological role of it remains enigmatic. We suggest that the association of microglia with blood vessels 24 h post MCAO and the succeeding phagocytosis of EC components are indicative of an active breakdown of tight junctions [30] and the BBB by microglia.

Indeed, permeabilization of the BBB following cerebral ischemia has been reported in mammals [6, 33]. The opening of the BBB in the ischemic brain is associated with blood vessel remodeling and angiogenesis in a VEGF-dependent manner [69]. This biphasic event consists of an early phase 4 h after stroke and a late phase occurring 24–48 h after the ischemic insult [32, 47]. The early permeability phase [58] coincides with a peak expression of VEGF, the earliest marker of vascular remodeling [15, 54], in the ischemic penumbra [53]. At 24 h after the insult, EC activation markers such as EGFL7 [50], PDGF-B [3], vWF [66], and ICAM-1 [24] are upregulated and, indeed, we detected the expression of all four markers in blood vessels of the ischemic penumbra at this time point, which is indicative of the early stage of BBB breakdown. In order to test for the disintegration of the BBB, we analyzed for proteins and cells that have been associated with BBB breakdown. Pharmacological and genetic evidence indicated that MMP-9 is required for angiogenesis in response to brain ischemia [34, 45]. Further, microglia are considered to be a major source of the protein in human specimens [56]. Indeed, we found MMP-9 to be upregulated in the penumbra 24–72 h after the insult. Classical markers of BBB breakdown are the release of blood serum components (e.g., serum albumin, fibrinogen, IgG), Evans blue, or neutrophils from blood vessels into the brain parenchyma. All of these hallmarks were observed 24–72 h post MCAO in our model, indicating a breakdown of the BBB at this time point. Remarkably, at 72 h post reperfusion, vascular structures in the penumbra were in part no longer present, indicating that

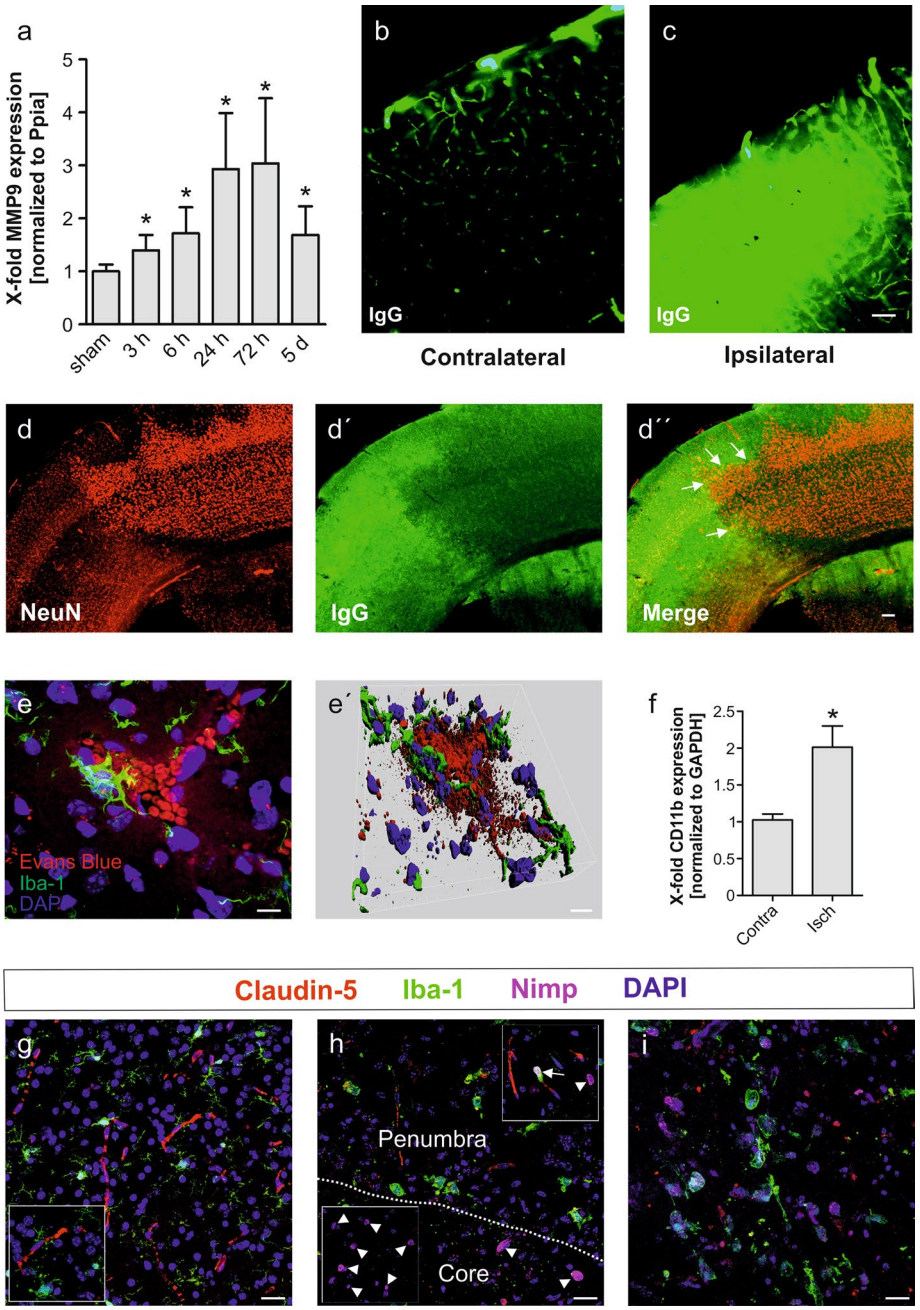

Fig. 6 MCAO induces BBB breakdown in the penumbra. **a** MCAO induced a significant upregulation of the metalloprotease MMP-9 in the penumbra (mean ± SEM, $n \geq 6$, $^*p < 0.05$). **b**–**d** Extravasation of IgG from leaky blood vessels, 24 h post MCAO in the **b** contralateral or **c** ipsilateral cerebral cortex with respect to the vessel occlusion. *Bars* represent 10 µm. **d** Double immunostaining using antibodies specific to the neuronal marker NeuN or **d′** IgG illustrating neuronal degeneration as well as the leakage of blood vessels in the stroke area. **d″** *Arrows* indicate the colocalization of extravasated IgG and cortical neurons in the penumbra. *Bars* represent 100 µm. **e** Microglia (Iba-1), blood plasma extravasation (Evans blue) and cell nuclei (DAPI) were detected by immunohistochemistry of brain sections of MCAO-treated animals 24 post reperfusion. Microglia associated with the still perfused blood vessels (see erythrocytes) during their disintegration, as shown by the faint cloud of Evans blue around the tube. **e′** The 3D reconstruction highlights the close interaction of microglia and perfused blood vessel. *Bars* represent 10 µm. **f** qRT-PCR analysis revealed a threefold increase in the amount of CD11b-positive immune cells detected in the ipsilateral hemisphere as compared to the contralateral site (mean ± SEM, $n \geq 6$, $^*p < 0.05$). Immunohistochemical staining of blood vessels (claudin-5), microglia (Iba-1), neutrophils (Nimp), and cell nuclei (DAPI) of the **g** contra- or **h** ipsilateral hemisphere of MCAO-treated animals 24 h post reperfusion revealed microglia activation and association with vascular structures as well as extravasation of neutrophils into the penumbra, which were observed intravascularly (*arrows*) and extravascularly (*arrowheads*). **i** 72 h post reperfusion, microglia were still activated and neutrophils detected in the penumbra but blood vessels were fully degraded. *Bars* represent 50 µm

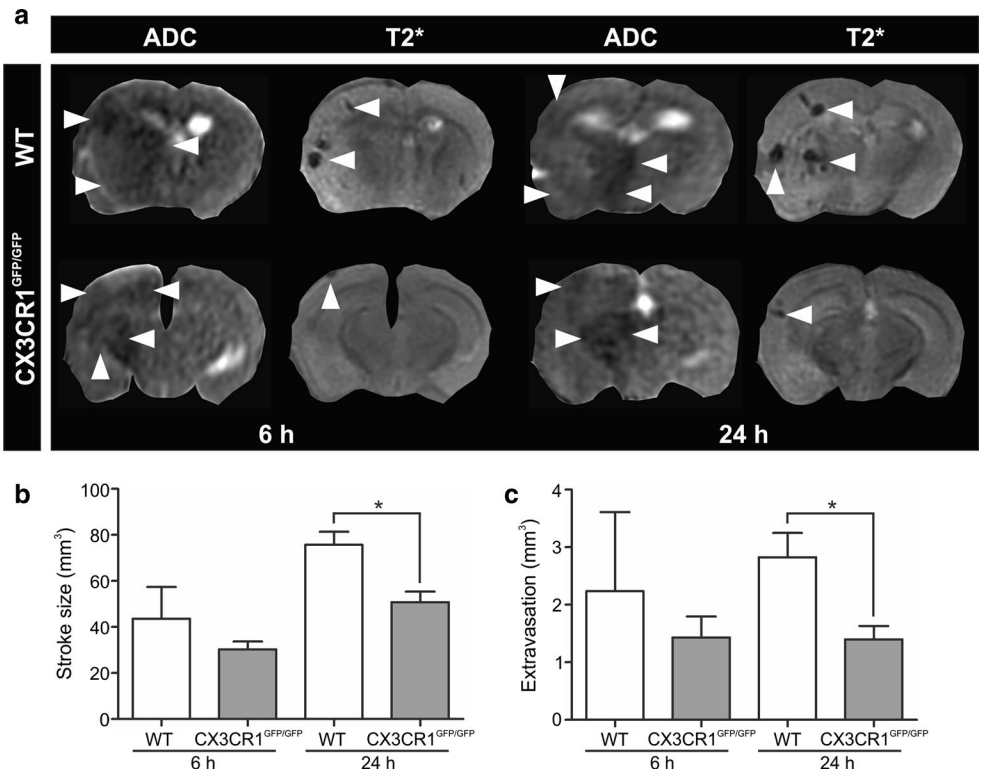

Fig. 7 Magnetic resonance imaging of mouse brains after MCAO. **a** Apparent diffusion coefficient (ADC) maps of diffusion-weighted imaging (DWI) and T2*-weighted imaging of mouse brains following MCAO (6 or 24 h) in coronal orientation. Hypointense areas represent restricted diffusion of stroke (ADC) as well as local bleeding (T2*) in WT and CX3CR1$^{GFP/GFP}$ mice (*arrowheads*). **b** Quantification of stroke size as measured by the volume (mm^3) of diffusion restriction on ADC maps or **c** the volume (mm^3) of contrast media extravasation (T1-weighted imaging) revealed a significant reduction of both parameters by approximately 50 % 24 h post reperfusion in CX3CR1$^{-/-}$ mice (mean ± SEM, $n = 3$, $^*p < 0.05$)

activated microglia contributed to the disintegration and degradation of blood vessels in this area. Intraparenchymal neutrophils were observed 72 h post reperfusion; however, the amount in the penumbra was low as compared to the core (Fig. 6h), which is in agreement with previous publications [14, 25] and supports the role of microglia in blood vessel breakdown.

Evidently, disintegration of blood vessels was not only restricted to the core of the stroke but also occurred in the neighboring tissue. Perivascular microglia were mostly observed in the ischemic penumbra and, therefore, we wondered which molecular cues might attract microglia to local blood vessels. We hypothesized that, upon permeabilization of the vascular wall caused by the ischemic stroke, blood components may diffuse into the cerebral parenchyma. Serum components such as albumin or fibrinogen have been described as major stimulators of microglia [2, 70]. Recently, the deposition of fibrinogen in the cerebral parenchyma has been reported to induce the clustering of microglia along blood vessels as a consequence of BBB disintegration [10]. These fibrinogen deposits have been shown to precede the infiltration of circulating monocytes into the brain parenchyma [16]. Furthermore, fibrinogen-derived peptides were described as chemotactic cues for human monocytes a long time ago [55]. In order to test whether blood serum-derived proteins have the capacity to activate resident microglia, we applied purified albumin and fibrinogen to BV2 [19] and found that both types of proteins induced the migration of microglia cells in a dose-dependent manner. Furthermore, microglia activation markers such as the cytokines IL-1β or TNF-α were significantly upregulated. This is in line with a previous publication that identified fibrinogen as an activator of microglia that led to an increase in cell body size and phagocytic activity [2]. Likewise, incubation of murine N9 microglia cells with serum albumin promoted the secretion of cytokines such as IL-1β and TNF-α [70]. Activation of microglia was also observed upon stroke in vivo and we found the phagocytosis marker CD68 as well as the co-stimulatory molecule CD86 to be upregulated, which is in agreement with the phagocytosis and activation data described above.

Although neurological damage occurs within seconds to minutes upon vessel occlusion, ischemic injury continues for hours and days [46]. Current data imply a slow-burning and irreversible scenario in which ischemic stroke causes a reduction in blood flow in blood vessels of the penumbra leading to hypoxia and upregulation of VEGF in the early subacute phase 4–6 h following stroke [42, 50, 53]. VEGF triggers an angiogenesis response that causes the disintegration of local EC and the extravasation of blood serum components like albumin or fibrinogen, which recruit nearby microglia that phagocytize the now activated EC and support the breakdown of the BBB in the late subacute phase 6–24 h after stroke. Blood flow in the affected blood vessels and in tubes connected to these vessels drops, which leads to an activation of microglia [44]. This process evolves

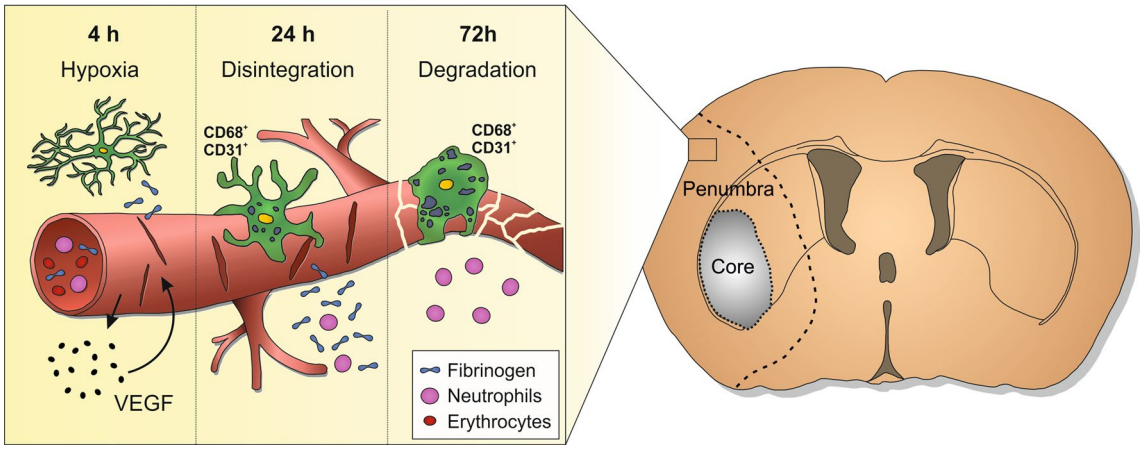

Fig. 8 Model of stroke-induced and microglia-mediated blood vessel destruction. Upon ischemic stroke, blood vessels in the core are destroyed but are potentially salvable in the penumbra. Untreated, hypoxia in these vessels triggers the upregulation of VEGF 4 h post insult, which activates the endothelium and renders the BBB partially permissive. Release of blood serum components such as fibrinogen leads to an activation of local microglia, which are recruited to blood vessels and contribute to their disintegration by the phagocytosis of EC and EC-components ($CD68^+/CD31^+$ microglia). Enlarged vessel damage allows for the extravasation of neutrophils and further blood serum components, which in turn activate more microglia and thereby contribute to the expansion of the damage in the neighboring ischemic penumbra along the tubular network. At 72 h post insult, blood vessel degradation is complete and remaining vessel debris is cleared by microglia and the invading immune cells

along the vascular network until a larger part of the ischemic penumbra is irreversibly damaged, but only an early restoration of blood flow can stop the evolving tissue damage in stroke [40, 46]. In the final delayed phase of stroke, immune cells such as lymphocytes and neutrophils invade the brain parenchyma and cause secondary inflammatory effects [21].

We present an alternative scenario that is compatible with previous data, but which includes the contribution of microglia and, crucially, allows for the possibility of halting the "slow-burning" damage in the early subacute phase. We found that microglia remove ECs from the process by phagocytosis (Fig. 8) and, as a consequence, the endothelium is irreversibly damaged and blood vessels regress resulting in tissue loss in the penumbra. As a matter of fact, loss-of-microglia-function studies using $CX3CR1^{GFP/GFP}$ animals revealed a reduction in stroke size and blood vessel extravasation by about half, which is in agreement with previous reports [12]. Our model also extends to peripheral macrophages, which cannot be distinguished from microglia using the methods applied in this manuscript. It fits well to the kinetics observed in patients, where brain damage caused by stroke gradually gets worse within the first 24 h post insult [21, 40, 46] and leads to BBB permeability as measured by the invasion of macrophages labeled with ultra-small superparamagnetic iron oxide into the brain parenchyma after 24 h [57]. Furthermore, targeting early BBB disruption has been shown to mediate neurovascular protection upon ischemic stroke [52]. In summary, the data above suggest the inhibition of microglial activation as an approach to decrease tissue damage in patients within the first 24 h post ischemic stroke in order to keep as many blood vessels intact as possible and to favor tissue repair in the ischemic penumbra over injury [39].

Acknowledgments We thank Heike Ehrengard, Christin Liefländer, Christine Oswald, and Andreas Zymny for their excellent technical assistance and Darragh O'Neill for proofreading the manuscript. This work was supported by the Foundation Rhineland-Palatinate to FZ, by the German Research Foundation (DFG) via the collaborative research center 1080, projects A3 (MHHS) and B6 (MKS+FZ), DFG FOR1336 (AW) as well as the DFG Grant SCHM 2159/2-1 to MHHS.

Conflict of interest The authors declare no competing financial interests.

References

1. Abdullah N, Voronovitch L, Taylor S, Lippmann S (2003) Olanzapine and quick-response hyperglycemia. Psychosomatics 44:175–176
2. Adams RA, Bauer J, Flick MJ et al (2007) The fibrin-derived gamma377-395 peptide inhibits microglia activation and suppresses relapsing paralysis in central nervous system autoimmune disease. J Exp Med 204:571–582
3. Arimura K, Ago T, Kamouchi M et al (2012) PDGF receptor beta signaling in pericytes following ischemic brain injury. Curr Neurovasc Res 9:1–9
4. Asahi M, Wang X, Mori T et al (2001) Effects of matrix metalloproteinase-9 gene knock-out on the proteolysis of blood-brain barrier and white matter components after cerebral ischemia. J Neurosci 21:7724–7732
5. Astrup J, Symon L, Branston NM, Lassen NA (1977) Cortical evoked potential and extracellular K+ and H+ at critical levels of brain ischemia. Stroke 8:51–57

6. Belayev L, Busto R, Zhao W, Ginsberg MD (1996) Quantitative evaluation of blood-brain barrier permeability following middle cerebral artery occlusion in rats. Brain Res 739:88–96
7. Carmeliet P, De Smet F, Loges S, Mazzone M (2009) Branching morphogenesis and antiangiogenesis candidates: tip cells lead the way. Nat Rev Clin Oncol 6:315–326
8. Cunningham CL, Martinez-Cerdeno V, Noctor SC (2013) Microglia regulate the number of neural precursor cells in the developing cerebral cortex. J Neurosci 33:4216–4233
9. Davalos D, Grutzendler J, Yang G et al (2005) ATP mediates rapid microglial response to local brain injury in vivo. Nat Neurosci 8:752–758
10. Davalos D, Ryu JK, Merlini M et al (2012) Fibrinogen-induced perivascular microglial clustering is required for the development of axonal damage in neuroinflammation. Nat Commun 3:1227
11. del Zoppo GJ, Milner R, Mabuchi T et al (2007) Microglial activation and matrix protease generation during focal cerebral ischemia. Stroke 38:646–651
12. Denes A, Ferenczi S, Halasz J, Kornyei Z, Kovacs KJ (2008) Role of CX3CR1 (fractalkine receptor) in brain damage and inflammation induced by focal cerebral ischemia in mouse. J Cereb Blood Flow Metab 28:1707–1721
13. Denes A, Ferenczi S, Halasz J, Kornyei Z, Kovacs KJ (2008) Role of CX3CR1 (fractalkine receptor) in brain damage and inflammation induced by focal cerebral ischemia in mouse. J Cereb Blood Flow Metab 28:1707–1721
14. Enzmann G, Mysiorek C, Gorina R et al (2013) The neurovascular unit as a selective barrier to polymorphonuclear granulocyte (PMN) infiltration into the brain after ischemic injury. Acta Neuropathol 125:395–412
15. Ferrara N, Gerber HP, LeCouter J (2003) The biology of VEGF and its receptors. Nat Med 9:669–676
16. Floris S, Blezer EL, Schreibelt G et al (2004) Blood-brain barrier permeability and monocyte infiltration in experimental allergic encephalomyelitis: a quantitative MRI study. Brain 127:616–627
17. Furlan M, Marchal G, Viader F, Derlon JM, Baron JC (1996) Spontaneous neurological recovery after stroke and the fate of the ischemic penumbra. Ann Neurol 40:216–226
18. Gelderblom M, Leypoldt F, Steinbach K et al (2009) Temporal and spatial dynamics of cerebral immune cell accumulation in stroke. Stroke 40:1849–1857
19. Girard S, Brough D, Lopez-Castejon G, Giles J, Rothwell NJ, Allan SM (2013) Microglia and macrophages differentially modulate cell death after brain injury caused by oxygen-glucose deprivation in organotypic brain slices. Glia 61:813–824
20. Heiss WD (2000) Ischemic penumbra: evidence from functional imaging in man. J Cereb Blood Flow Metab 20:1276–1293
21. Heiss WD (2012) The ischemic penumbra: how does tissue injury evolve? Ann N Y Acad Sci 1268:26–34
22. Iadecola C, Anrather J (2011) The immunology of stroke: from mechanisms to translation. Nat Med 17:796–808
23. Jin R, Yang G, Li G (2010) Inflammatory mechanisms in ischemic stroke: role of inflammatory cells. J Leukoc Biol 87:779–789
24. Justicia C, Panes J, Sole S et al (2003) Neutrophil infiltration increases matrix metalloproteinase-9 in the ischemic brain after occlusion/reperfusion of the middle cerebral artery in rats. J Cereb Blood Flow Metab 23:1430–1440
25. Kalimo H, del Zoppo GJ, Paetau A, Lindsberg PJ (2013) Polymorphonuclear neutrophil infiltration into ischemic infarctions: myth or truth? Acta Neuropathol 125:313–316
26. Karperien A, Ahammer H, Jelinek HF (2013) Quantitating the subtleties of microglial morphology with fractal analysis. Front Cell Neurosci 7:3
27. Katsura K, Kristian T, Siesjo BK (1994) Energy metabolism, ion homeostasis, and cell damage in the brain. Biochem Soc Trans 22:991–996
28. Kitamura Y, Takata K, Inden M et al (2004) Intracerebroventricular injection of microglia protects against focal brain ischemia. J Pharmacol Sci 94:203–206
29. Kitamura Y, Yanagisawa D, Inden M et al (2005) Recovery of focal brain ischemia-induced behavioral dysfunction by intracerebroventricular injection of microglia. J Pharmacol Sci 97:289–293
30. Knowland D, Arac A, Sekiguchi KJ et al (2014) Stepwise recruitment of transcellular and paracellular pathways underlies blood-brain barrier breakdown in stroke. Neuron 82:603–617
31. Kopatz J, Beutner C, Welle K et al (2013) Siglec-h on activated microglia for recognition and engulfment of glioma cells. Glia 61:1122–1133
32. Kuntz M, Mysiorek C, Petrault O et al (2014) Stroke-induced brain parenchymal injury drives blood-brain barrier early leakage kinetics: a combined in vivo/in vitro study. J Cereb Blood Flow Metab 34:95–107
33. Kuroiwa T, Ting P, Martinez H, Klatzo I (1985) The biphasic opening of the blood-brain barrier to proteins following temporary middle cerebral artery occlusion. Acta Neuropathol 68:122–129
34. Lee CZ, Xu B, Hashimoto T, McCulloch CE, Yang G-Y, Young WL (2004) Doxycycline suppresses cerebral matrix metalloproteinase-9 and angiogenesis induced by focal hyperstimulation of vascular endothelial growth factor in a mouse model. Stroke 35:1715–1719
35. Li T, Pang S, Yu Y, Wu X, Guo J, Zhang S (2013) Proliferation of parenchymal microglia is the main source of microgliosis after ischaemic stroke. Brain 136:3578–3588
36. Li X, Blizzard KK, Zeng Z, DeVries AC, Hurn PD, McCullough LD (2004) Chronic behavioral testing after focal ischemia in the mouse: functional recovery and the effects of gender. Exp Neurol 187:94–104
37. Livak KJ, Schmittgen TD (2001) Analysis of relative gene expression data using real-time quantitative PCR and the 2(-Delta Delta C(T)) method. Methods 25:402–408
38. Lloyd-Jones D, Adams R, Carnethon M et al (2009) Heart disease and stroke statistics–2009 update: a report from the American Heart Association Statistics Committee and Stroke Statistics Subcommittee. Circulation 119:480–486
39. Lo EH (2008) A new penumbra: transitioning from injury into repair after stroke. Nat Med 14:497–500
40. Lo EH, Dalkara T, Moskowitz MA (2003) Mechanisms, challenges and opportunities in stroke. Nat Rev Neurosci 4:399–415
41. Madinier A, Bertrand N, Mossiat C et al (2009) Microglial involvement in neuroplastic changes following focal brain ischemia in rats. PLoS One 4:e8101
42. Marti HJ, Bernaudin M, Bellail A et al (2000) Hypoxia-induced vascular endothelial growth factor expression precedes neovascularization after cerebral ischemia. Am J Pathol 156:965–976
43. Martin RL, Lloyd HG, Cowan AI (1994) The early events of oxygen and glucose deprivation: setting the scene for neuronal death? Trends Neurosci 17:251–257
44. Masuda T, Croom D, Hida H, Kirov SA (2011) Capillary blood flow around microglial somata determines dynamics of microglial processes in ischemic conditions. Glia 59:1744–1753
45. Morancho A, Hernández-Guillamon M, Boada C et al (2013) Cerebral ischaemia and matrix metalloproteinase-9 modulate the angiogenic function of early and late outgrowth endothelial progenitor cells. J Cell Mol Med 17:1543–1553
46. Moskowitz MA, Lo EH, Iadecola C (2010) The science of stroke: mechanisms in search of treatments. Neuron 67:181–198
47. Nag S, Kapadia A, Stewart DJ (2011) Review: molecular pathogenesis of blood-brain barrier breakdown in acute brain injury. Neuropathol Appl Neurobiol 37:3–23
48. Neumann H, Kotter MR, Franklin RJ (2009) Debris clearance by microglia: an essential link between degeneration and regeneration. Brain 132:288–295

49. Nikolic I, Plate KH, Schmidt MHH (2010) EGFL7 meets miRNA-126: an angiogenesis alliance. J Angiogenes Res 2:9
50. Nikolic I, Stankovic ND, Bicker F et al (2013) EGFL7 ligates alphavbeta3 integrin to enhance vessel formation. Blood 121:3041–3050
51. Nimmerjahn A, Kirchhoff F, Helmchen F (2005) Resting microglial cells are highly dynamic surveillants of brain parenchyma in vivo. Science 308:1314–1318
52. Pillai DR, Shanbhag NC, Dittmar MS, Bogdahn U, Schlachetzki F (2013) Neurovascular protection by targeting early blood-brain barrier disruption with neurotrophic factors after ischemia-reperfusion in rats. J Cereb Blood Flow Metab 33:557–566
53. Plate KH, Beck H, Danner S, Allegrini PR, Wiessner C (1999) Cell type specific upregulation of vascular endothelial growth factor in an MCA-occlusion model of cerebral infarct. J Neuropathol Exp Neurol 58:654–666
54. Pugh CW, Ratcliffe PJ (2003) Regulation of angiogenesis by hypoxia: role of the HIF system. Nat Med 9:677–684
55. Richardson DL, Pepper DS, Kay AB (1976) Chemotaxis for human monocytes by fibrinogen-derived peptides. Br J Haematol 32:507–513
56. Rosell A, Ortega-Aznar A, Alvarez-Sabín J et al (2006) Increased brain expression of matrix metalloproteinase-9 after ischemic and hemorrhagic human stroke. Stroke 37:1399–1406
57. Saleh A, Schroeter M, Ringelstein A et al (2007) Iron oxide particle-enhanced MRI suggests variability of brain inflammation at early stages after ischemic stroke. Stroke 38:2733–2737
58. Sandoval KE, Witt KA (2008) Blood-brain barrier tight junction permeability and ischemic stroke. Neurobiol Dis 32:200–219
59. Schilling M, Besselmann M, Muller M, Strecker JK, Ringelstein EB, Kiefer R (2005) Predominant phagocytic activity of resident microglia over hematogenous macrophages following transient focal cerebral ischemia: an investigation using green fluorescent protein transgenic bone marrow chimeric mice. Exp Neurol 196:290–297
60. Schmidt MHH, Bicker F, Nikolic I et al (2009) Epidermal growth factor-like domain 7 (EGFL7) modulates Notch signalling and affects neural stem cell renewal. Nat Cell Biol 11:873–880
61. Sierra A, Abiega O, Shahraz A, Neumann H (2013) Janus-faced microglia: beneficial and detrimental consequences of microglial phagocytosis. Front Cell Neurosci 7:6
62. Sierra A, Encinas JM, Deudero JJ et al (2010) Microglia shape adult hippocampal neurogenesis through apoptosis-coupled phagocytosis. Cell Stem Cell 7:483–495
63. Stence N, Waite M, Dailey ME (2001) Dynamics of microglial activation: a confocal time-lapse analysis in hippocampal slices. Glia 33:256–266
64. Strasser GA, Kaminker JS, Tessier-Lavigne M (2010) Microarray analysis of retinal endothelial tip cells identifies CXCR4 as a mediator of tip cell morphology and branching. Blood 115:5102–5110
65. Ueyama T, Lennartz MR, Noda Y et al (2004) Superoxide production at phagosomal cup/phagosome through beta I protein kinase C during Fc gamma R-mediated phagocytosis in microglia. J Immunol 173:4582–4589
66. Yang JP, Liu HJ, Liu XF (2010) VEGF promotes angiogenesis and functional recovery in stroke rats. J Invest Surg 23:149–155
67. Yenari MA, Xu L, Tang XN, Qiao Y, Giffard RG (2006) Microglia potentiate damage to blood-brain barrier constituents: improvement by minocycline in vivo and in vitro. Stroke 37:1087–1093
68. Zhang J, Defelice AF, Hanig JP, Colatsky T (2010) Biomarkers of endothelial cell activation serve as potential surrogate markers for drug-induced vascular injury. Toxicol Pathol 38:856–871
69. Zhang ZG, Zhang L, Jiang Q et al (2000) VEGF enhances angiogenesis and promotes blood-brain barrier leakage in the ischemic brain. J Clin Invest 106:829–838
70. Zhao TZ, Xia YZ, Li L et al (2009) Bovine serum albumin promotes IL-1beta and TNF-alpha secretion by N9 microglial cells. Neurol Sci 30:379–383